Journal of The Electrochemical Society, **153** (7) F153-F159 (2006)
0013-4651/2006/153(7)/F153/7/$20.00 © The Electrochemical Society

Effect of Water Addition in the Spray Solution on the Synthesis of Zirconium–Aluminum Oxide Films Prepared by the Pyrosol Process

M. Bizarro,[a] J. C. Alonso,[a] J. Fandiño,[b] and A. Ortiz[a,z]

[a]*Instituto de Investigaciones en Materiales, and* [b]*Instituto de Física, Universidad Nacional Autonoma de Mexico, Coyoacán 04510, México D.F., Mexico*

Zirconium–aluminum oxide films were deposited by the pyrosol process using metallic acetylacetonates. The effect of addition of water, in volumes from 20 to 1000 μL per 30 mL of the starting solution on the synthesis of the films deposited is analyzed. X-ray diffraction spectra show that the films are of amorphous phase. The deposition rate decreases while the aluminum incorporated in the films increases as the water volume is augmented. These behaviors are related to the action that the water molecules have on the reactants, promoting the decomposition of the reactants even at relatively low temperatures, resulting in carbon-free and transparent films. Refractive index acquires values around 1.85. Fourier transform infrared spectra show absorption bands related with vibration of Zr–O and Al–O bonds forming a ternary oxide. The energy gap determined has values of the order of 5.85 eV, which is between the values of zirconium oxide and aluminum oxide. Current–voltage characteristics in metal–oxide–metal structures show that the effect of water is to diminish the leakage current density, although its magnitude is large. From capacitance measurements, the dielectric constant has values of the order of 23.8, which is higher than that calculated for films prepared by the same process without the addition of water. The dielectric loss factor calculated from the capacitance–voltage characteristics has high values, in agreement with the large leakage current densities observed.
 [DOI: 10.1149/1.2203200]

Manuscript submitted November 10, 2005; revised manuscript received March 22, 2006. Available electronically May 22, 2006.

The dielectric properties of silicon dioxide used as a gate insulator in metal-oxide-semiconductor field effect transistors (MOSFETs) represent the key element enabling the scaling of complementary metal-oxide-semiconductor (CMOS) integrated circuits. Amorphous silicon dioxide gate insulator grown on the surface of silicon substrates is thermodynamically and electrically stable, forming a high-quality Si/SiO_2 interface with a midgap interface state density of $\sim 10^{10}$ cm^2 eV and breakdown electric fields as high as 15 MV/cm. However, the manufacturing trend is toward ultralarge integration circuits, which has forced the channel length and gate dielectric thickness to decrease rapidly ($\sim$1.5–1.8 nm). This fact indicates that SiO_2 thinner than the above values cannot be used as the gate dielectric in CMOS devices because the leakage current density and power consumption are unacceptably high.[1,2] The trend in reducing the lateral dimensions of devices has as a consequence a reduction of the capacitance of the involved MOS structures; thus, insulators with higher dielectric constant (k) should be used to compensate. Then, to prevent a high leakage current density and to keep the area of devices small and maintain the same gate capacitance, thicker films of materials with higher dielectric constant are required.[3] Some binary and ternary oxides prepared as thin films using different deposition processes have been suggested as possible alternative dielectrics to replace SiO_2, such as Ta_2O_5, TiO_2, Al_2O_3, ZrO_2, Y_2O_3, La_2O_3, HfO_2, and barium strontium titanate.[4-11] Some of the above-mentioned binary oxides have lower crystallization temperatures than those used in several steps of the CMOS preparation process. In general, crystallization of the insulator gate induces high leakage current densities through the grain boundaries, so in order to stabilize an amorphous phase of the insulator gate, the addition of SiO_2 or Al_2O_3 has been necessary.[12-16]

Among the binary metallic oxides mentioned above, the preparation of high-quality Al_2O_3 and ZrO_2 thin films by the ultrasonic spray pyrolysis method has been reported.[17,18] In those cases, the microstructural analyses of deposited aluminum oxide films show that all of them are amorphous for any set of deposition conditions. ZrO_2 films deposited at substrate temperatures higher than 525°C show a cubic or monoclinic crystalline phase, depending on the deposition conditions. In both cases the current density vs applied electric field characteristics indicate that the breakdown electric field has values of at least 6 MV/cm. The effect of the process conditions on the synthesis of zirconium–aluminum oxide thin films prepared by the pyrosol method was recently reported.[19] The spray solution was made using acetylacetonates of zirconium and aluminum dissolved in pure methyl alcohol. In that case, the aluminum concentration incorporated in the deposited films increases as the magnitude of the substrate temperature, the carrier gas flow rate, and the aluminum concentration in the spray solution increase.

In this work, in order to get a better understanding of the chemical reactions determining the synthesis of zirconium–aluminum oxide films deposited by the ultrasonic spray pyrolysis method, we report the effect of the addition of water in the spray solution on the structure, relative chemical composition, and some electric properties of the deposited films.

Experimental

The zirconium–aluminum oxide films were deposited by the pyrosol process, which is a well-known method to produce oxide films.[20] The starting solution was 0.025 M zirconium acetylacetonate (ZrAcAc) with 5 atom % aluminum acetylacetonate (AlAcAc) added [(Al/Zr)s ratio equal to 0.05 in solution] dissolved in as-purchased pure methanol, as was earlier reported.[19] Further spraying solutions were prepared adding water to the above-mentioned solution in the following volumes (Vw): 0 (ZAA1), 20 (ZAA2), 50 (ZAA3), 100 (ZAA4), 250 (ZAA5), 500 (ZAA6), 750 (ZAA7), and 1000 (ZAA8) μL per each 30 mL of starting solution. The substrate temperature of 475°C, as well as the carrier and the director gas flow rates of 3.5 and 7 L/min, were kept constant. The gas used was filtered air in all cases. The deposition time was varied from 5.5 for the sample without water up to 21.0 min for the sample with water added in the proportion of 1000 μL/30 mL, in order to deposit films with measurable thickness. The films were deposited onto (100) n-type silicon single-crystal slices with 200 Ω cm electrical resistivity. These substrates were chemically cleaned with P etch solution [H_2O (300 mL), HF (15 mL), HNO_3 (10 mL)] in order to remove the native oxide from their surfaces. Clear fused quartz slices and Corning 7059 glass slices covered with a transparent conducting oxide (TCO) film were also used. These substrates were ultrasonically cleaned with trichloroethylene, acetone, and methanol. For electrical measurements, in order to make an electric contact with the TCO films a small area of these films was covered with a Pyrex cover before the sample films deposition. For electrical characterization aluminum dots with a diameter of 0.12 cm were deposited by vacuum thermal evaporation onto these samples through a metallic

[z] E-mail: aortiz@servidor.unam.mx

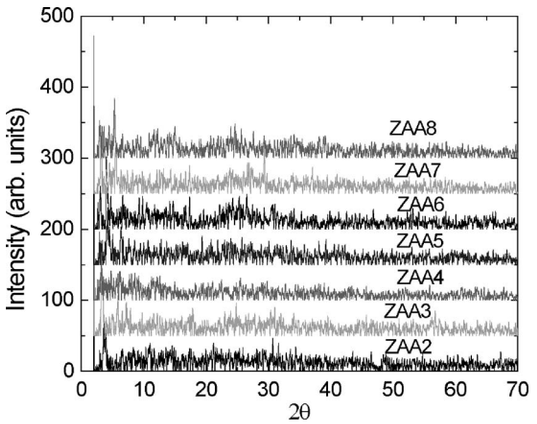

Figure 1. X-ray diffraction spectra for films deposited with different volumes of water added to the starting solution. There are no peaks that indicate some crystalline structure.

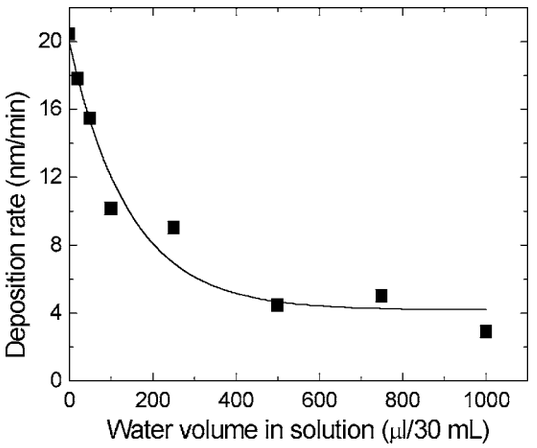

Figure 2. Decreasing exponential variation of the deposition rate for increasing water volume added to the starting solution.

mask to form metal–oxide–metal structures (MOM). The crystallinity of the films deposited onto the fused quartz slices substrates was analyzed by X-ray diffraction measurements with a Siemens D-5000 diffractometer using a Cu Kα wavelength (0.154056 nm) for an integration time of 14 h. The thickness and index of refraction were measured with a manual Gaertner 117A ellipsometer using the 632 nm line of a He–Ne laser in the films deposited onto single-crystalline Si slices. Infrared spectra were obtained for these samples with a Fourier transform infrared (FTIR) 205 Nicolet spectrophotometer in the range of 400–4000 cm^{-1}. Optical transmission and reflection were measured on the films deposited on clear fused quartz substrates by means of a double-beam spectrophotometer UNICAM UV-300, with air in the reference beam. Relative chemical composition analyses of films deposited onto c-Si were performed by X-ray photoelectron spectroscopy (XPS) measurements using a UHV system VG-Scientific Microtech Multilab ESCA2000 with a CLAM4 MCD detector analyzer. A Mg Kα X-ray source was used ($h\nu$ = 1253.6 eV) with a 20 mA beam intensity and a polarized anode at 15 kV. The spectra were obtained at 55° with respect to the surface normal with a constant energy step of E_0 = 20 eV. The analysis was performed using the software SDPv4.1 and the sensitivity factor reported by Scofield. The pressure was kept constant at 1×10^{-8} mb during measurements. Current–voltage curves of the MOM structures were obtained with a Keithley 230 programmable voltage source and a Keithley 485 picoammeter. The capacitance of these structures was obtained using a GenRad 1657 RLC Digibridge meter at 1 kHz.

Results

Figure 1 shows the X-ray diffraction spectra for samples deposited with different volumes of water added to the starting solution as indicated. These spectra were obtained using an integration time of 14 h in all cases. The spectra do not show clear features associated with crystalline phases. Because the substrate temperature used during the deposition was lower than that in which crystalline zirconium oxide can be produced by spray pyrolysis, it was expected that the deposited films were amorphous. The deposition rate was calculated as the quotient of the thickness of the films and the deposition time used. Figure 2 shows the variation of the deposition rate (*Rd*) as a function of the volume of water added to the starting solution. This variation can be described by means of a decreasing exponential function, with a trend toward an almost constant value of *Rd*. This fact indicates that the water added to the starting solution has a strong effect on the chemical reactions determining the *Rd*. This behavior explains the necessary variation of deposition time. Figure 3 shows the depth profile of chemical composition obtained by XPS for samples prepared without water (Fig. 3a) and with 250 μL/30 mL (Fig. 3b) and 1000 μL/30 mL (Fig. 3c) water added to the starting solution. It can be observed that in profiles 3a and b the relative concentration of zirconium is higher than that of aluminum, but in profile 3c the concentrations of zirconium and aluminum are almost equal. These results indicate that the effect of the water added in the starting solution is in favor of the incorporation of aluminum oxide in the deposited material. This fact explains the result of Fig. 2, because the aluminum concentration in the starting solution is only 5 atom % of that of zirconium, giving place to a reduction of *Rd* with a trend toward a constant value. From these XPS results the Al/Zr ratio values were calculated, taking into account the Al and Zr concentrations. These measurements were carried out for the same sputter time in all samples. The Al/Zr ratio values are shown in Fig. 4 as a function of the water volume added in the starting solution. It is observed that the Al/Zr ratio increases monotonically as *Vw* increases, in agreement with the results of the chemical composition depth profiles as was expected. A similar behavior was previously observed in zirconium–aluminum oxide films deposited by the same process when the Al/Zr ratio in the starting solution was augmented.[19] However, the trend observed in the present case can probably be explained based on the effect that the added water has on the source materials and on the chemical reactions producing the solid thin films. The refractive index (n) measured for the zirconium–aluminum oxide films deposited onto single-crystalline silicon wafers has an almost constant value around 1.85 for all the volumes of water added in the starting solution, as shown in Fig. 5. This behavior is similar to that observed in zirconium–aluminum oxide films deposited by the pyrosol process,[19] where the substrate temperature, the carrier gas flow rate, and the aluminum concentration in the starting solutions were varied.

Figure 6 shows the FTIR spectra for samples deposited with 0, 50, 250, and 750 μL of water added to the starting solution, respectively. All these spectra have small but well-defined absorption bands. The bands located at 404, 460, and 570 cm^{-1} can be related with vibration modes of Zr–O bonds. Meanwhile, the band located around 664 can be related with the vibration mode of the Al–O bonds. It should be clarified that the location of these bands is near to those reported for stoichiometric ZrO_2 and Al_2O_3 compounds.[21-26] In all spectra there is a small absorption band located at around 1075 cm^{-1} which is related to a silicon oxide film developed at the interface during deposition of the zirconium-aluminum oxide film onto the silicon substrate.

From the optical transmission and reflection spectra the absorption coefficient was calculated using the method developed by Swanepoel.[27] As the deposited films were amorphous for all depo-

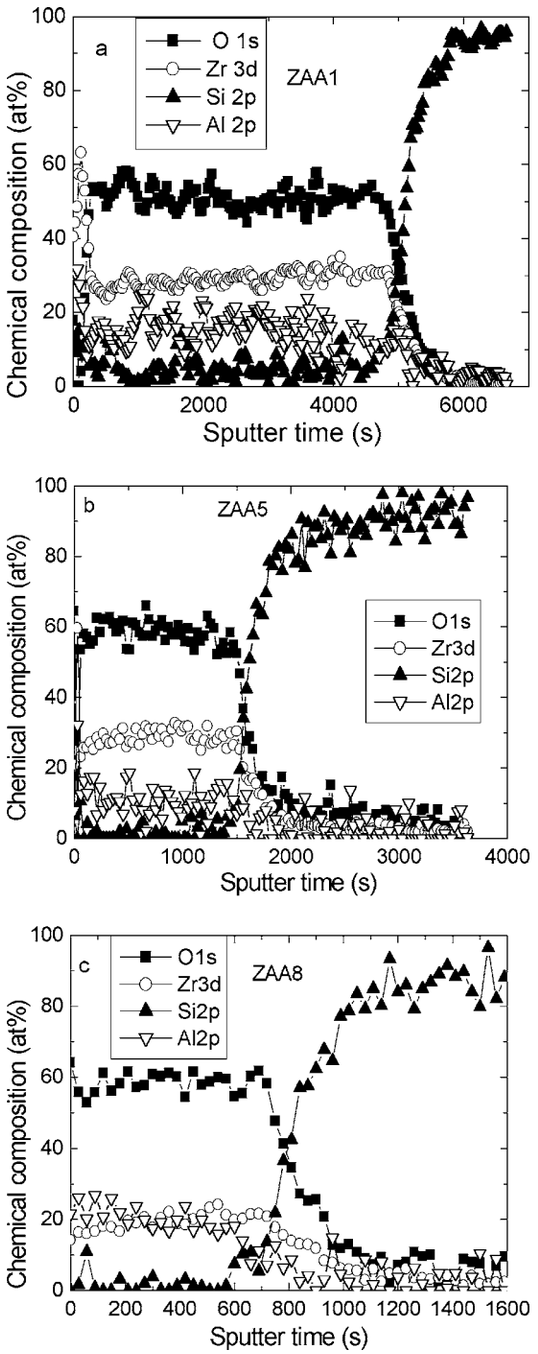

Figure 3. XPS depth profile of zirconium–aluminum oxide films prepared with (a) 0 (ZAA1), (b) 250 (ZAA5), and (c) 1000 (ZAA8) μL of water added to 30 mL of the starting solution.

sition conditions, energy bandgap (*Eg*) values were calculated using the Tauc model.[28] In Fig. 7 the dependence of the energy bandgap on the volume of water added to the starting solution is shown. For low values of *Vw*, the energy bandgap acquires values around 5.81 eV, whereas for higher values of *Vw*, which give higher values of the Al/Zr ratio, *Eg* is almost constant with a value of the order of 5.88 eV. All *Eg* values calculated in the present case are in the range determined by the energy bandgap values obtained for zirconium oxide films (5.47 eV) and aluminum oxide films ($Eg > 6.2$ eV) prepared by the pyrosol process.[18,29]

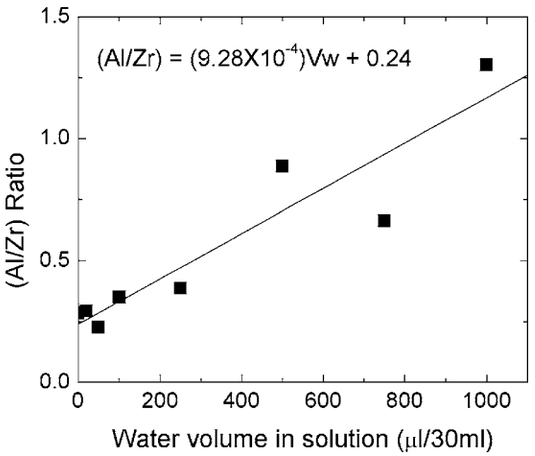

Figure 4. Variation of the Al/Zr ratio as a function of the water volume added to the starting solution. This result indicates that the AlAcAc decomposition rate is higher than that of ZrAcAc.

Figure 8 shows the current density vs applied electric field characteristics of MOM structures for three values of *Vw*. The thickness of the ternary oxide used in these structures are 101.0 (ZAA3), 72.1 (ZAA5), and 85.0 (ZAA7) nm, respectively. It is observed that for same values of applied electric field, the current density has lower values when more water is added to the starting solution, although it appears that for high *Vw* values these curves are very similar, with values of current density of the same order of magnitude for all the range of values of applied electric field. The shape of these curves appears to indicate that the leakage current densities are large. From capacitance measurements on the same MOM structures (with the same values of thickness for the ternary oxide film), the dielectric constant and the dielectric loss factor (tan δ) of the oxide layer were calculated considering a parallel plate capacitor. Figure 9 shows the variation of *k* and tan δ as a function of the volume of water added to the starting solution. In this figure the error bars represent a dispersion of the values of *k* calculated for at least five MOM structures produced on the same Corning 7059 glass slices covered with a TCO film substrate. The dielectric constant has lower values for capacitors prepared with starting solutions with small *Vw* than those obtained in samples prepared with large *Vw*. Although it can be

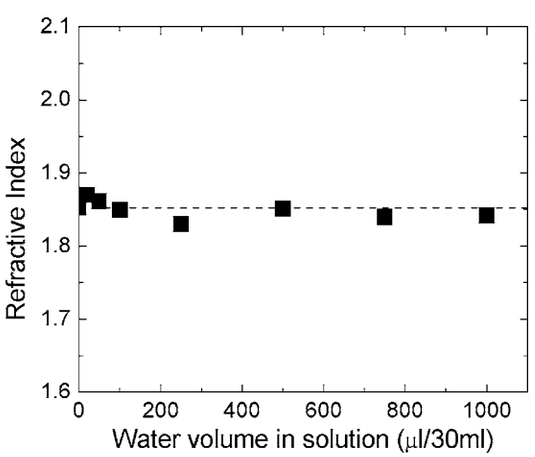

Figure 5. Refractive index of the Zr–Al–O films deposited for all the volumes of water added to the starting solution. All values are around 1.85.

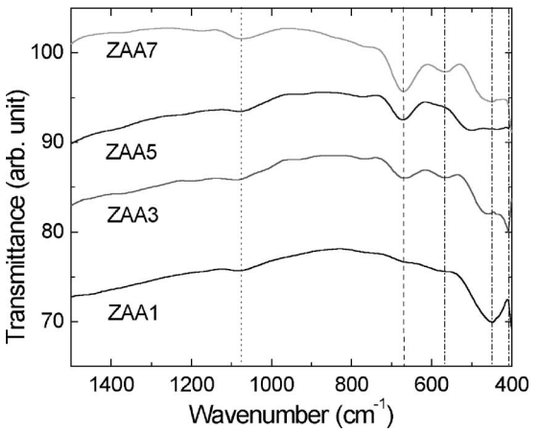

Figure 6. FTIR spectra for zirconium–aluminum oxide films deposited using different values of *Vw*. The location of the absorption bands associated with (–·–·–), Zr–O: 404, 460, and 570 cm^{-1}, (---) Al–O: 664 cm^{-1}, and (···) Si–O 1075 cm^{-1}, vibration modes are indicated.

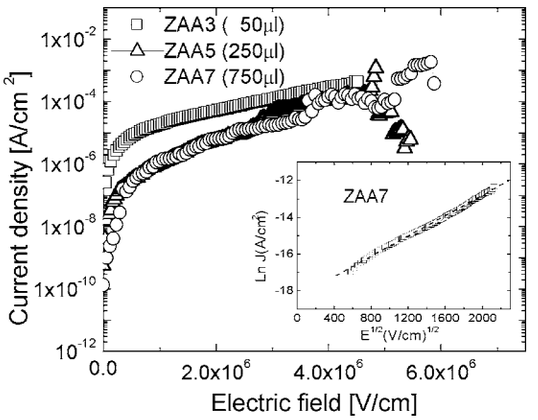

Figure 8. Current density–applied electric field characteristics of MOM structures for oxide films prepared with different *Vw* values. The thickness of the ternary oxide films used in these structures are 101.0 (ZAA3), 72.1 (ZAA5), and 85.0 (ZAA7) nm, respectively. The current density decreases at least by one order of magnitude for increasing *Vw*.

considered that the dielectric constant value is almost constant, it does not have a strong dependence on *Vw*. The dielectric loss factor has high values.

Discussion

It was expected that all deposited films were of amorphous phase given the relatively low substrate temperature used during deposition and the aluminum acetylacetonate added in the starting solution. The substrate temperature used for film deposition is lower than that where crystalline zirconium oxide can be produced.[18] Besides, the aluminum incorporated in these films, forming a ternary compound with zirconium and oxygen, also enhances the amorphous phase of the deposited films. It has been reported that films deposited with aluminum acetylacetonate added to the starting solution in the same concentration as in the present case results in the incorporation of aluminum in the deposited films with values around 20 atom % with respect to the zirconium concentration.[19] This higher value appears to indicate that the oxidation rate of aluminum radicals is higher than that of the zirconium radicals, both of which are generated by the decomposition of the source materials. The incorporation of this relatively high concentration of aluminum in the zirconium oxide induces the stabilization of the amorphous phase of the deposited films.[30]

The results of Fig. 2-4 show the strong effect of the addition of relatively small volumes of water to the starting solution, with (*i*) a deposition rate decreasing toward an almost constant value and (*ii*) the almost linear increase of the Al/Zr ratio values as *Vw* is augmented. In order to explain these variations, it should be considered that in the deposition process the starting solution is atomized by an ultrasonic beam, generating small drops which are transported by the carrier gas toward the reaction chamber, where the heated substrate is located. In its transit toward the surface of the heated substrate the solvent of the starting solution is evaporated, giving place to an atmosphere that contains methanol and water vapors. It has been published that aluminum oxide films deposited by low-pressure metallorganic chemical vapor deposition (CVD) process, at given temperatures and using dialkylacetylacetonates as source materials in an inert atmosphere (N_2 gas) without water vapor or oxygen gas, have black color. Chemical composition analyses show that the deposited material is formed by metallic suboxides and organic radicals from the material source decomposition. Generally, these films are very rich in carbon (more than 10% of their weight).[31] Films formed by completely oxidized metallic elements without the incorporation of organic species can be obtained in high-temperature processes or in a low-temperature process by adding water vapor to the atmosphere during deposition.[17,32] Also, in studies of the reactions of bis(2,4-pentanedionato)lead(II) and water vapor[33] and tris(2,4-

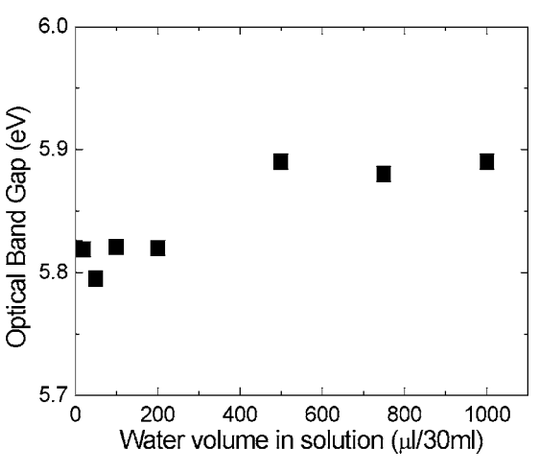

Figure 7. Optical bandgap for Zr–Al–O films as a function of *Vw*. The optical bandgap has a small increment related with a high aluminum concentration incorporated in the films.

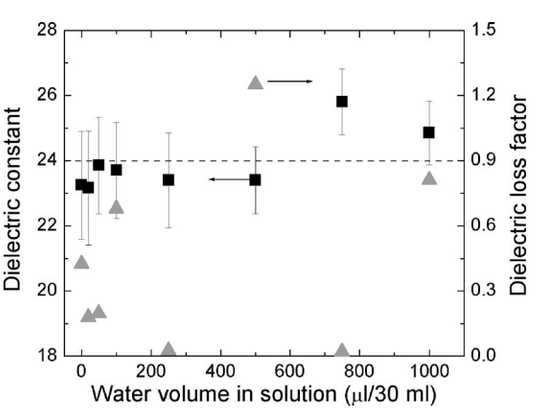

Figure 9. Dielectric constant (■) and dielectric loss factor (▲) variation as a function of *Vw*. The dielectric constant acquires values of the order of those reported for zirconium oxide films.

pentanedionato) aluminum and water vapor[34] similar behaviors were observed. The existence of several chemical species in the vapor phase during the decomposition process was analyzed by gas chromatography, mass spectroscopy, and FTIR measurements. In those works several pathway chemical reactions are proposed to obtain metallic oxides as products. The CVD process is carried out at a given temperature, then the pyrolysis of the source material represent a direct decomposition pathway producing organic species like C_5H_6O and intermediate species, such as $Al(C_5H_7O_2)OH$, in the case of aluminum 2,4-pentanedionate. If the reaction with water is considered, the same intermediate species are produced as well as the organic species 2,4-pentanedione ($C_5H_8O_2$). Considering that aluminum acetylacetonate $[Al(C_5H_7O_2)_3]$ is adsorbed on the surface of the substrate during the reaction to produce aluminum oxide, the overall reaction would be

$$2Al(C_5H_7O_2)_3(sur) + 3H_2O(g) \rightarrow Al_2O_3(s) + 6C_5H_8O_2(g) \quad [1]$$

Rhoten and De Vore obtained a value for the activation energy for this reaction of $+245 \pm 5$ kJ/mol,[34] taking into account that the heat of formation of $Al_2O_3(s)$ has a value of -1675.7 kJ/mol.[36] In the case of lead oxide, using bis(2,4-pentanedionato)lead(II) the obtained value for the activation energy of the reaction is $+105 \pm 5$ kJ/mol,[33] with the heat of formation value of PbO(s) of -219.4 kJ/mol.[35] An important result of these studies is that the pathways of the chemical reactions with lowest energy correspond to those in which the reactions between the metallic acetylacetonate with water are involved. These reactions occurred at relatively low temperatures and produce carbon-free metallic oxide films.

In the present work a possible overall reaction to produce $ZrO_2(s)$ using zirconium acetylacetonate $Zr(C_5H_7O_2)_4$ with water would be

$$Zr(C_5H_7O_2)_4(sur) + 2H_2O(g) \rightarrow ZrO_2(s) + 4C_5H_8O_2(g) \quad [2]$$

The heat of formation of $Al_2O_3(s)$ can be obtained considering values published in Ref. 36. Taking into account that in the present case the substrate temperature was 475°C, the value calculated was similar to the above mentioned of the order -1675 kJ/mol. The value calculated for the heat of formation of $ZrO_2(s)$, considering published data in Ref. 36, is -946 kJ/mol. The difference between the values of the heat of formation for $Al_2O_3(s)$ and that for the $ZrO_2(s)$ indicates that the pathway of the chemical reaction to produce aluminum oxide needs lower energy. This result infers that the chemical reaction rate forming $Al_2O_3(s)$ is higher than that for $ZrO_2(s)$. The difference between these chemical reaction rates should be increased as the volume of water added to the starting solution is augmented.

Results obtained in some studies on metallic acetylacetonates decomposition have established that if the concentration of water is low enough the activation energy for decomposition of metallic acetylacetonates would approach that determined for direct pyrolysis decomposition, 100 kJ/mol for AlAcAc.[34,37] Similarly, if the concentration of water is high enough, the activation energy for decomposition of metallic acetylacetonates would approach that determined for the hydrolysis reaction, 28 kJ/mol for AlAcAc.[34,38] In an intermediate case, for metallic acetylacetonate decomposition both processes contribute and the activation energy determined would be an intermediate value. Then the pathway reaction needing lower energy dominates at low temperatures if an excess of water vapor is present. The zirconium and aluminum acetylacetonate concentrations in the starting solution, in the present work, are 4.51×10^{20} molecules of ZrAcAc and 2.26×10^{19} molecules of AlAcAc in 30 mL of starting solution. The number of water molecules calculated for each volume of water added to the starting solution varies from 6.68×10^{20} (20 μL/30 mL) up to 3.34×10^{22} (1000 μL/30 mL). When the ratio of the number of water molecules to the number of aluminum acetylacetonate molecules is calculated, it reaches values from 29.6 up to 1478. Meanwhile, the ratio of the number of water molecules to the number of zirconium acetylacetonate molecules reaches values from 1.48 up to 74. Given these values, it could be considered that for AlAcAc the decomposition conditions goes from low concentration toward high enough concentration of water, and for ZrAcAc the deposition conditions appear to be always near to low enough concentrations of water. Moreover, these variations can be reinforced by the presence of oxygen from the air used as carrier and director gas. Then the chemical reaction producing Al_2O_3 dominates at high water concentration. As a result of the above analysis, the water added to the starting solution establishes two conditions: (*i*) for small values of volume of water added to the starting solution, the activation energies for aluminum and zirconium acetylacetonates decomposition are determined by direct pyrolysis. Given the large concentration of ZrAcAc in comparison with that of AlAcAc, the deposited films are formed by a material that has a larger concentration of zirconium oxide radicals than that of aluminum oxide radicals. This high concentration of ZrAcAc and its decomposition process result in a relatively high deposition rate. (*ii*) For large values of volume of water added to the starting solution, the activation energy for aluminum acetylacetonate decomposition is determined by a hydrolysis reaction and the activation energy for zirconium acetylacetonate decomposition is mainly determined by direct pyrolysis. These differences in activation energies result in a larger generation rate of metallic aluminum species than that of metallic zirconium species. Taking into account this fact and the values of heat of formation for aluminum and zirconium oxides, there is a larger generation rate of aluminum oxide radicals than that of zirconium oxide radicals. This result could indicate that if it is considered, the relatively low concentration of aluminum acetylacetonate in the starting solution and that the zirconium oxidation is carried out by the pyrolysis process, such that in the pathway of the chemical reaction the formation of volatile species related with zirconium could be generated, then the deposition rate for the zirconium aluminum oxide films should decrease. All the abovementioned effects determining the variations are observed in the results shown in Fig. 2-4. In depth-profile chemical composition obtained by XPS measurements, carbon was detected only on the surface of the films analyzed, in agreement with results earlier reported.[17,32]

The almost constant behavior of the refractive index can be seen as the result of two parts, one with low values of *Vw* and the other with high values of *Vw*. In the first case, low values of *Vw* give high deposition rates and *n* acquires values which can be determined by two mechanisms. (*i*) Given the high deposition rate the deposited films have a relatively low density which results in low values of *n*. This effect of low density resulting in a decrease of refractive index has been observed in several metallic oxides prepared by different processes.[39,40] (*ii*) The concentration of aluminum incorporated in the films is already higher than that used in the starting solution, contributing to the decrease in the value of *n*. In the second case, for high values of *Vw*, the deposition rate acquires an almost constant low value, giving place to a densification effect of deposited films. As it was explained above, the addition of high volumes of water to the starting solution induce a more efficient decomposition of AlAcAc over the ZrAcAc, with higher concentrations of aluminum incorporated in the films that make the Al/Zr ratio acquire values higher than 1. These effects can be balanced, resulting in films with an almost constant refractive index, taking values between 1.81 and 1.89. A similar behavior has been reported for the ternary oxide ($TaTiO_x$), where the refractive index acquires values near to that of the Ta_2O_5 for samples with equal concentrations of metallic oxides, indicating that a simple interpolation of the indices of the pure oxides is not correct.[41]

The results of FTIR spectroscopy show that the absorption bands associated with Al–O and Zr–O vibration modes correspond to stoichiometric Al_2O_3 and ZrO_2 compounds. The small differences should be related with the presence of both metallic oxides in the deposited films. Changes in the frequencies of vibration modes of Si–O bonds due to the presence of bismuth atoms has been observed in the generation of bismuth silicate films formed by an interdiffu-

sion process between silicon dioxide and bismuth oxide.[42] Probably, a similar effect is responsible for the observed behavior. The presence of zirconium atoms near to Al–O bonds can induce small changes in the frequencies of its vibration modes due to its major atomic mass. Similarly, the presence of aluminum atoms near to Zr–O bonds can induce small changes in the frequencies of its vibration modes due to its smaller atomic mass. In this case the effect of the water added is to improve the dissociation of the organic molecules of the source materials (metallic acetylacetonates), resulting in better oxidation of the metallic atoms as they arrive to the heated surface of the substrate.

The behavior of the optical bandgap as a function of water volume added to the starting solution changes slightly for samples prepared with small values of *Vw* compared with those obtained with values of at least 500 μL. This is understandable if it is considered that for low values of *Vw* the aluminum oxide concentration in the films has its lowest values, with the Al/Zr ratio having values lower than 0.5. Perhaps at those *Vw* values some organic species, from the incomplete decomposition of the source materials, can be incorporated in the deposited films. For great values of *Vw* the aluminum oxide concentration in the films acquires its highest values, because the water added to the starting solution may induce an almost complete decomposition of the AlAcAc, which results in Al/Zr ratio having values as high as 1.25, resulting in a trend toward wider optical bandgap.

From the current density vs electric field characteristics, the effect of addition of water to the starting solution is to reduce at least by 1 order of magnitude the current density for electric fields up to 4 MV/cm. However, given the general form of these curves, with a trapping ledge, it appears that there should be a high density of charge carrier traps in the volume of the films. This could be explained by electron injection into interfacial traps associated with zirconium atoms.[43] The shape of these curves also appears to indicate that the leakage current density is large in all the analyzed samples. If a plot of natural logarithm of the current density vs the square root of the electric field is made, a linear dependence is observed (inset of Fig. 8). This could indicate that the leakage current behavior is consistent with the Schottky emission model.[44] However, more work is necessary to clarify this point. It can be seen that for applied electric fields higher than 4.5 MV/cm, the current density shows an irregular variation. This behavior is due to the damage of the aluminum electrode because the high current established through the MOM structure at those electric fields induces the oxidation of the aluminum electrode. This oxidation is observable with naked eye.

The behavior observed for the dielectric constant as a function of *Vw* can be explained if it is considered that a balancing effect is achieved, in a similar way as happened for the refractive index. For low values of *Vw* the aluminum oxide concentration in the films is relatively small, but probably the deposited films are formed by a low-density material, giving place to relatively low values of *k*. Meanwhile, for large values of *Vw* there should be a better decomposition of the source materials, at least of the AlAcAc, and also a better oxidation of the metallic atoms, giving place to materials deposited with high values of *k*. The deposition rate for the latest films has its lowest values. This fact might permit the deposition of denser films, which induces the high *k* values measured. These *k* values are higher than those calculated in zirconium–aluminum oxide films prepared by the same process at similar conditions but without water addition in the starting solution. The high values of tan δ calculated are in agreement with the large values of the leakage current density observed in the current density-applied electric field characteristics. In order to get zirconium–aluminum oxide films with good electrical characteristics, more work is necessary.

Conclusions

The addition of relatively small volumes of water to the starting solution for deposition of zirconium–aluminum oxide films by the pyrosol process, using acetylacetonates of zirconium and aluminum, has a strong effect on the chemical reactions for oxidation of Zr and Al atoms, giving place to the increase of the aluminum concentration incorporated in the deposited films as *Vw* is augmented. Water molecules promote a more efficient decomposition of the organometallic source materials, which generate metallic atoms that are completely oxidized. The incorporation of aluminum atoms in the network of ZrO_2 stabilizes the amorphous phase obtained at the substrate temperature used. The location of absorption bands associated with Zr–O and Al–O bonds in the infrared spectra show small shifts in comparison with those observed in stoichiometric aluminum oxide and zirconium oxide, indicating that the presence of the metallic atoms with different atomic mass induce changes in the frequency of the vibration modes of the metal–oxygen bonds. The addition of water in the starting solution has little effect on the refractive index and the energy bandgap values of the Zr–Al–O films because their calculated values are in the ranges determined by the values of ZrO_2 and Al_2O_3. A similar behavior is obtained for the magnitude of the dielectric constant that has values around 23.8, which is of the order of several values reported for zirconium oxide films, although the dielectric loss factor has large values, in agreement with the high leakage current density observed. All these properties indicate that the material forming the deposited films is a ternary oxide. The effect that the water addition has on the I–V characteristics is to reduce at least by one order the magnitude of the leakage current density. However, the electrical properties were obtained in samples without any thermal postdeposition process.

Acknowledgments

The authors thank to L. Huerta, S. Jimenez, and L. Baños for technical support. This work has been partially supported by DGAPA-UNAM under project no. IN109803.

National Autonomous University of Mexico assisted in meeting the publication costs of this article.

References

1. G. D. Wilk, R. M. Wallace, and J. M. Anthony, *J. Appl. Phys.*, **89**, 5243 (2001).
2. A. I. Kingon, J. P. Maria, and S. K. Streiffer, *Nature (London)*, **406**, 1032 (2000).
3. E. B. O. da Rosa, J. Morais, R. P. Pezzi, L. Miotti, and I. J. R. Baumvol, *J. Electrochem. Soc.*, **148**, G695 (2001).
4. E. Deloffre, L. Montés, G. Ghibaudo, S. Bruyère, S. Blonkowski, S. Bécu, M. Gros-Jean, and S. Crémer, *Microelectron. Reliab.*, **45**, 925 (2005).
5. A. Ritz, *Surf. Coat. Technol.*, **174–175**, 651 (2003).
6. E. P. Gusev, M. Copel, E. Cartier, I. J. R. Baumvol, C. Drug, and M. A. Gribelyuk, *Appl. Phys. Lett.*, **76**, 176 (2000).
7. Y. Z. Hu and S. P. Tay, *J. Vac. Sci. Technol. B*, **19**, 1706 (2001).
8. J. J. Chambers and G. N. Parsons, *Appl. Phys. Lett.*, **77**, 2385 (2000).
9. H. Yamada, T. Shimizu, A. Kurokawa, K. Ishii, and E. Suzuki, *J. Electrochem. Soc.*, **150**, G429 (2003).
10. K. P. Bastos, J. Morais, L. Miotti, R. P. Pezzi, G. V. Soarez, I. J. R. Baumvol, H. H. Tseng, R. I. Hedge, and P. J. Tobin, *Appl. Phys. Lett.*, **81**, 507 (2002).
11. M. Vehkamäki, T. Hänninen, M. Ritala, M. Leskela, T. Sajavaara, E. Rauhala, and J. Keinonen, *Chem. Vap. Deposition*, **7**, 75 (2001).
12. W. J. Qi, R. Nieh, E. Dhamarajan, B. H. Lee, Y. Jeon, L. Kang, K. Onishi, and J. C. Lee, *Appl. Phys. Lett.*, **77**, 1704 (2000).
13. J. Morais, E. B. O. da Rosa, L. Miotti, R. P. Pezzi, I. J. R. Baumvol, A. L. P. Rotondaro, M. J. Bevan, and L. Colombo, *Appl. Phys. Lett.*, **78**, 2446 (2001).
14. C. S. Desu, P. C. Joshi, and S. B. Desu, *J. Electroceram.*, **10**, 209 (2003).
15. W. F. A. Besling, E. Young, T. Conard, C. Zhao, R. Carter, W. Vandervorst, M. Caymax, S. De Gendt, M. Heyns, J. Maes, M. Tuominen, and S. Haukka, *J. Non-Cryst. Solids*, **303**, 123 (2002).
16. J. H. Jun and D. J. Choi, *Jpn. J. Appl. Phys., Part 1*, **43**, 7576 (2004).
17. A. Ortiz and J. C. Alonso, *J. Mater. Sci.: Mater. Electron.*, **13**, 7 (2002).
18. A. Ortiz, J. C. Alonso, and E. Haro-Poniatowski, *J. Electron. Mater.*, **34**, 150 (2005).
19. M. Bizarro, J. C. Alonso, and A. Ortiz, *J. Electrochem. Soc.*, **152**, 179 (2005).
20. M. Langlet and J. C. Jaubert, in *Chemistry of Advanced Materials, Pyrosol Process or the Pyrolysis of an Ultrasonically Genrated Aerosol*, C. N. R. Rao, Editor, p. 55, Blackwell Scientific, Oxford, England (1993).
21. R. A. Nyquist and R. O. Kagel, in *Infrared Spectra of Inorganic Compounds* (3800-45 cm^{-1}), Vol., 4, The Dow Chemical Company, pp. 209–211, Academic Press, Midland, MI (1997).
22. T. Maruyama and A. Arai, *Appl. Phys. Lett.*, **60**, 322 (1992).
23. Y. C. Kim, H. H. Park, J. S. Chun, and W. J. Lee, *Thin Solid Films*, **237**, 57 (1994).
24. F. F. Bentley, L. D. Smithson, and A. L. Rozek, in *Infrared Spectra and Characteristics Frequencies* ≈700–300 cm^{-1}*; A Collection of Spectra, Interpretation and Bibliography*, p. 1564, John Wiley and Sons, New York (1968).
25. L. A. Pérez-Maqueda and E. Matijevic, *J. Mater. Res.*, **12**, 3286 (1997).

26. R. N. Tauber, A. C. Dunbri, and R. E. Caffrey, *J. Electrochem. Soc.*, **118**, 747 (1971).
27. R. Swanapoel, *J. Phys. E*, **16**, 1214 (1983).
28. S. Adachi, in *Optical Properties of Crystalline and Amorphous Semiconductors*, Chap. 4, Kluwer Academic Publishers, Boston, MA (1999).
29. A. Ortiz, J. C. Alonso, V. Pankov, A. Huanosta, and E. Andrade, *Thin Solid Films*, **368**, 74 (2000).
30. R. B. van Dover, D. V. Lang, M. L. Green, and L. Manchada, *J. Vac. Sci. Technol. A*, **19**, 2779 (2001).
31. G. A. Battiston, G. Carta, R. Gerbasi, M. Porchia, L. Rizzo, and G. Rossetto, *J. Phys. IV*, **9**(8), 675 (1999).
32. A. G. Nasibulin, L. I. Shurygina, and E. I. Kauppinen, *Colloid J.*, **67**, 5 (2005).
33. M. A. Crouch and T. C. DeVore, *Chem. Mater.*, **8**, 32 (1996).
34. M. C. Rhoten and T. C. De Vore, *Chem. Mater.*, **9**, 1757 (1997).
35. M. W. Chase, Jr., C. A. Davies, J. R. Downey, Jr., D. J. Frurip, R. A. McDonald, and A. N. Syverud, *J. Phys. Chem. Ref. Data*, **1985**, 14.
36. *CRC Handbook of Chemistry and Physics*, 67th Ed., R. C. Weast, Editor, p. D33, CRC Press, Boca Raton, FL (1986–1987).
37. T. Maruyama and S. Arai, *Appl. Phys. Lett.*, **69**, 322 (1992).
38. V. G. Minkina, *Inorg. Mater.*, **29**, 1400 (1993).
39. L. Castañeda, J. C. Alonso, A. Ortiz, E. Andrade, J. M. Saniger, and J. G. Bañuelos, *Mater. Chem. Phys.*, **77**, 938 (2002).
40. A. Ortiz, J. C. Alonso, and C. Falcony, *J. Electrochem. Soc.*, **140**, 3014 (2993).
41. A. Ritz, *Surf. Coat. Technol.*, **174–175**, 651 (2003).
42. O. Rico-Fuentes, E. Sánchez-Aguilera, C. Velásquez, R. Ortega-Alvarado, J. C. Alonso, and A. Ortiz, *Thin Solid Films*, **478**, 96 (2005).
43. G. Lucovsky, G. B. Rayner, Jr., D. Kang, G. Appel, R. S. Johnson, Y. Zhang, D. E. Sayers, H. Ade, and J. L. Whitten, *Appl. Phys. Lett.*, **79**, 1775 (2001).
44. Y. W. Kwon, Y. Li, Y. W. Heo, and D. P. Norton, *Thin Solid Films*, **489**, 99 (2005).